Eur Biophys J (2002) 31: 136–144
DOI 10.1007/s00249-001-0201-3

ARTICLE

László Oroszi · András Dér · Pál Ormos

Theory of electric signals of membrane proteins in three dimensions

Received: 29 June 2001 / Revised: 22 November 2001 / Accepted: 22 November 2001 / Published online: 30 January 2002

Abstract Transmembrane ion pumps are often investigated experimentally by photoelectric measurements in model systems. In addition to the most widely used systems based on model membranes, a fundamentally different class is represented by the so-called suspension methods. In this technique the electric signal is measured on a bulk suspension of oriented ion pumps in the form of a displacement current. On this system, electric and spectroscopic experiments can be performed simultaneously. Using the information from both types of measurements, and utilizing the three-dimensional nature of the system, it is possible to follow the intramolecular charge motions in all three spatial directions. The derivable dipole moment changes associated with conformational transitions allow the verification of molecular dynamic models. In this work a theory is presented to describe the suspension method; samples with different symmetry properties and the possibilities of photoselection to obtain the desired three-dimensional information are analyzed.

Keywords Three-dimensional systems · Electric signals · Photoselection · Conformational changes · Membrane proteins

Introduction

Membrane-coupled electric processes play a crucial role in biological signal and energy transduction pathways. The electric potential difference across membranes is controlled by ion channels and pumps. Investigation of ion pumps is therefore one of the fundamental questions of bioenergetics.

L. Oroszi · A. Dér · P. Ormos (✉)
Institute of Biophysics of the Hungarian Academy of Sciences, Temesvári krt. 62, P.O. Box 521, 6726 Szeged, Hungary
E-mail: pali@nucleus.szbk.u-szeged.hu
Fax: +36-62-433133

Widely used methods for measuring membrane-coupled electric signals are different microelectrode techniques on native systems. Because of technical reasons, however, their application is not always feasible. For the effective investigation of ion pumps, in most cases, model systems had to be developed.

The basic requirement for the detection of electric signals in a model system is the creation of an electric asymmetry in the sample. The various measuring techniques can be characterized by the way of achievement of this asymmetry. Two basic categories can be distinguished.

First, an extremely widely used class is the model membrane system. Here, the principal component of the system is a membrane separating two electrically conductive regions. The membrane is fundamental in two aspects: it separates the two electrolyte compartments (both physically and electrically), and the ion pump under study is incorporated into this model membrane. The transmembrane ion movement is followed by electrodes immersed in the two compartments. Such model membrane systems have proven very effective in the study of ion transporters; several different versions have been elaborated (Drachev et al. 1974; Dancsházy and Karvaly 1976; Herrmann and Rayfield 1978; Hong and Montal 1979; Fahr et al. 1981; Trissl 1990). The basic property of all model membrane systems is that the structure is principally two dimensional and a single layer of pump is working. The geometry of the system is such that only the charge motion in the transmembrane direction, i.e. in the membrane normal, can be detected.

Subsequently, another branch of methods has been elaborated with fundamentally different characteristics: the so-called suspension methods (Keszthelyi and Ormos 1980). In this technique there is no integral model membrane structure as the principal component of the system. Here the electric measurement is done on a suspension of membrane fragments containing the ion pump (note that the membrane fragment has no function: it simply contains the protein). In this

case, the asymmetry needed for macroscopic electric signals is created by the orientation of the membrane fragments by an electric (or magnetic) field. The electric signal is measured as a displacement current in the suspension. It has to be pointed out here that this system is fundamentally a three-dimensional structure, and offers several advantages over the model membrane system owing to the fact that a bulk structure with a large number of pumps is investigated. First, the suspension methods allow the simultaneous measurement of optical signals associated with protein conformational changes, which is especially advantageous in kinetic investigations. In addition, owing to the 3D character there is a principal possibility to follow charge motions in all spatial directions, absolutely not possible in the 2D membrane model systems.

As already mentioned, orientation is achieved by an electric or magnetic field (Keszthelyi 1980; Dér et al. 1995). The orientation can be monitored by linear dichroism or light scattering (Keszthelyi 1980; Barabás et al. 1983). The oriented membrane fragments can be fixed by embedding them in a gel (Dér et al. 1985b), which renders possible the detection of electric signals over a wide range of environmental parameters. An alternative way for fixing oriented membranes is drying the suspension (Váró 1981). The operation of pump molecules can be synchronized, in light-driven systems by light, in other cases via chemical jumps. The suspension methods were first applied in the study of bacteriorhodopsin (bR), the simplest known ion pump in living organisms. Later, they were generalized to investigate other ion pumps or light-sensitive proteins (the Cl-pumping halorhodopsin, octopus rhodopsin, photosystem-I) (Dér et al. 1985a, 1992b; Govorunova et al. 1995; Ormos et al. 1996). Note that the so-called light-gradient method, originally developed for the investigation of the photosynthetic apparatus, can also be considered as a version of the suspension technique where the electric asymmetry is created by the exciting light itself (Witt and Zickler 1973; Fowler and Kok 1974; Trissl et al. 1982).

Figure 1 shows the general scheme of the measuring apparatus for the suspension methods. In those cases where both electric and absorption kinetic signals are available, a time correlation between the two types of traces can normally be established (Keszthelyi and Ormos 1980; Váró and Keszthelyi 1983; Dér et al. 1985b; Müller et al. 1991). Correlation of electric and absorption kinetic signals inspired the interpretation of the former as consequences of intramolecular charge displacements (Keszthelyi and Ormos 1980). Using some simplifying assumptions (first-order kinetics, unidirectional, unbranched photocycle, homogeneous dielectrics, etc.), conclusions on proton jumps associated with the transitions of the bR photocycle were derived from the kinetic photoelectric traces. In spite of the simple theory used at that time, the results were in agreement with the predictions from early structural data (Henderson et al. 1990). In his review, Trissl (1990) gave a more general formula for the evaluation of electric signals measured by the suspension methods, and later attempts were made to characterize the dielectric properties of the sample as well (Liu and Ebrey 1988).

In this paper we establish a theoretical background for the interpretation of the electric signals measured by the suspension techniques. The macroscopically detectable (photo)voltages are interpreted as the results of fast intramolecular charge displacements and the subsequent relaxation of the surrounding electrolyte. The theory renders it possible to calculate molecular dipole moment changes associated with the conformational transitions, based on the photoelectric measurement. This allows the verification of molecular dynamic models by comparing the theoretical and measured dipole moment changes of intermediates.

Interpretation of electric signals

The analysis is structured according to the symmetry properties of the sample. We follow the concept of demonstrating general features first, via simplified,

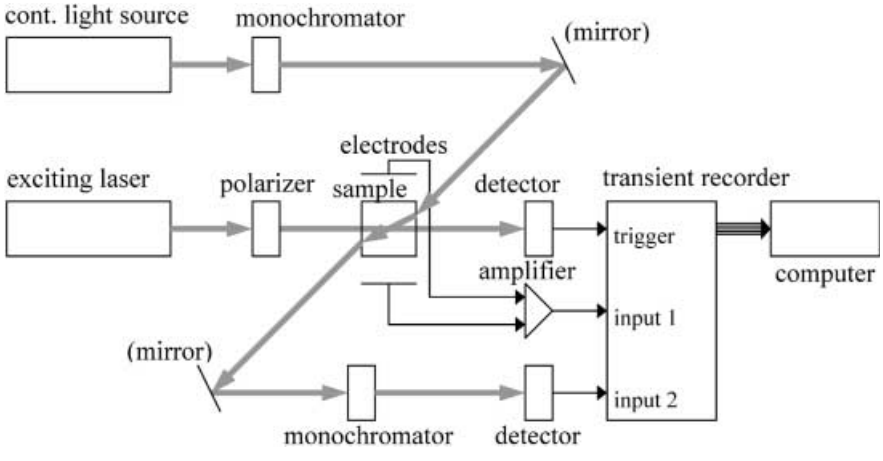

Fig. 1 Possible realization of the measuring system in the case of a light-triggered protein, utilizing photoselection

idealized cases (e.g. "sample of perfect direction"). The conclusions drawn by the help of these case studies provide the basis for the interpretation of electric measurements with the suspension methods on realistic samples (like oriented retinal proteins, e.g. bacteriorhodopsin, excited by linearly polarized light).

First, let us define the different types of samples being analyzed in our description. A common property of all samples is that they contain a macroscopic number of molecules rotationally fixed in the electrolyte. Categorization is made by the specific angular distribution of the molecules.

Sample of perfect direction

This is the simplest, theoretical case, in which the (macroscopic number of) molecules face in exactly the same direction.

Oriented samples

This sample is prepared according to Dér et al. (1985b). First, the molecules are oriented with a homogeneous electric field acting on their *permanent* dipoles (or on the permanent dipoles of the membrane fragments containing them). Then the angular distribution (Fig. 2a) resulting from the electric interaction and the rotational diffusion of the molecules is frozen using some fixation techniques. We call the theoretical case, where the orientation is ideal, the *sample of perfect orientation*.

Aligned samples

This sample is prepared according to Dér et al. (1995). Here the molecules are oriented with a homogeneous electric or magnetic field acting on their *induced* dipoles (or on the induced dipoles of the membrane fragments containing them). Then the angular distribution (Fig. 2b) is fixed. The theoretical case, where the alignment is ideal, is called the *sample of perfect alignment*.

In the next sections, we denote vector/matrix components by upper indices, with lower indices being used for qualitative distinction. We will use two coordinate systems: one assigned to the molecule and the other to the laboratory. Our analysis will reveal how molecular dipole moment changes generate macroscopic voltages detectable by electrode pairs aligned along the axes of the laboratory coordinate system.

Sample of perfect direction

As mentioned before, this sample contains a macroscopic number of proteins, perfectly directed, surrounded by an electrolyte. The molecules are undergoing conformational transitions between certain intermediates (the underlying process can be, for example, an ion pumping cycle of a transmembrane protein triggered by light). Let us consider a single molecule. The dipole moment of that in the ith intermediate state is denoted by μ_i^k (defined in the molecular coordinate system). We focus on the $i \rightarrow j$ intermediate transition, where the dipole moment of the molecule changes its value by $\mu_{ij}^k = \mu_j^k - \mu_i^k$ within a transition time t_T. Our theory handles typical cases, where the surrounding electrolyte compensates this μ_{ij}^k transient dipole rapidly (with relaxation time t_R) compared to the intermediate life times (t_L), and slowly compared to the intermediate transition time (t_T), so we can write:

$$t_T \ll t_R \ll t_L \tag{1}$$

Let us consider an $i \rightarrow j$ transition of a molecule occurring at $t = 0$. At the beginning, the total dipole moment function of the molecule + electrolyte system starts with a value proportional to $\mu_{ij}^k = \mu_j^k - \mu_i^k$ and

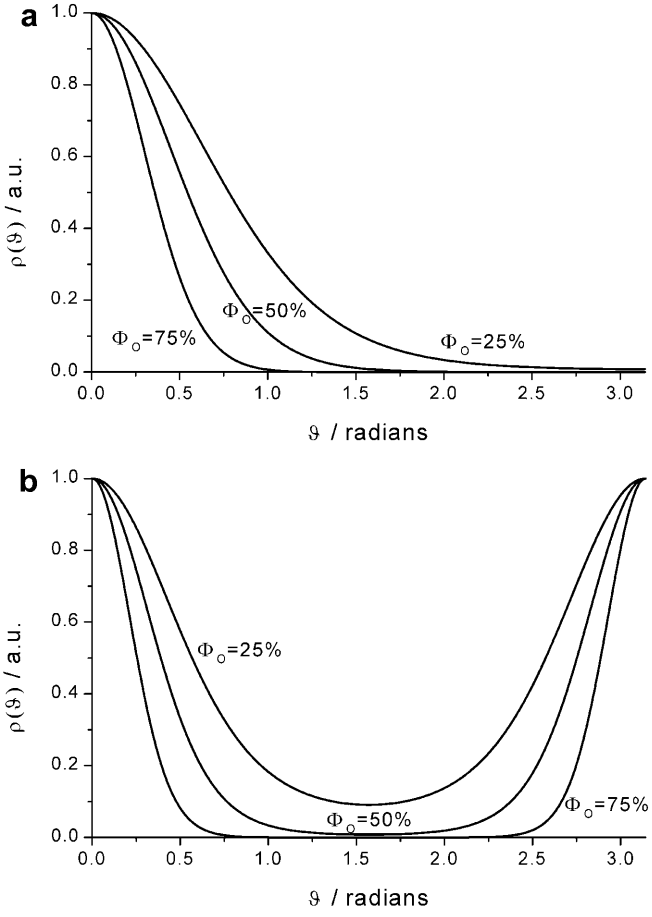

Fig. 2 The angular density function ($\rho(\vartheta)$) in the case of oriented (**a**) and aligned (**b**) samples. The angular distribution corresponds to the permanent (**a**) and induced (**b**) dipole-field interaction, where ϑ is the angle between the orienting/aligning field and the permanent/induced dipole vector, and Φ_0 is the orientation function (Barabás et al. 1983)

then it relaxes with a characteristic time t_R as the electrolyte compensates the dipole change. This total dipole moment function fluctuates due to individual ion motions, but the average of a sufficiently large number of the same transitions is well defined, and we denote it by $\tilde{\mu}^k_{ij}(t)$.

At a given time t the ith intermediate has a concentration of $x_i(t)$. Assuming first-order chemical reactions, the number of molecules undergoing an $i \rightarrow j$ transition at a given t is proportional to $x_i(t)$and k_{ij} (rate constant of the reaction). We can write for $\tilde{\mu}^k_{ij}(t)_\Sigma$, the total dipole moment function of the system (all molecules + electrolyte) induced by the $i \rightarrow j$ transition:

$$\tilde{\mu}^k_{ij}(t)_\Sigma \sim \int_0^t \tilde{\mu}^k_{ij}(t-t_0)k_{ij}x_i(t_0)\mathrm{d}t_0 \tag{2}$$

Using the assumptions for $\tilde{\mu}^k_{ij}(t)$ of a fast relaxation compared to the intermediate lifetimes and that the time integral of $\tilde{\mu}^k_{ij}(t)$ is proportional to μ^k_{ij}:

$$\begin{aligned}\int_0^t \tilde{\mu}^k_{ij}(t-t_0)k_{ij}x_i(t_0)\mathrm{d}t_0 &\cong \int_{t-t_R}^t \tilde{\mu}^k_{ij}(t-t_0)k_{ij}x_i(t_0)\mathrm{d}t_0 \\ &\cong k_{ij}x_i(t)\int_{t-t_R}^t \tilde{\mu}^k_{ij}(t-t_0)\mathrm{d}t_0 \\ &\sim k_{ij}x_i(t)\mu^k_{ij}\end{aligned} \tag{3}$$

Thus we obtain the following relation:

$$\tilde{\mu}^k_{ij}(t)_\Sigma \sim \mu^k_{ij}k_{ij}x_i(t) \tag{4}$$

Now let us calculate $\tilde{\mu}^k(t)_\Sigma$, the dipole moment function resulting from all of the $i \rightarrow j$ transitions in the system:

$$\begin{aligned}\tilde{\mu}^k(t)_\Sigma &= \sum_{i,j}\tilde{\mu}^k_{ij}(t)_\Sigma \sim \sum_{i,j}\mu^k_{ij}k_{ij}x_i(t) \\ &= \sum_{i,j}\left(\mu^k_j - \mu^k_i\right)k_{ij}x_i(t) \\ &= \sum_j \mu^k_j \sum_i k_{ij}x_i(t) - \sum_i \mu^k_i \sum_j k_{ij}x_i(t) \\ &= \sum_i \mu^k_i \sum_j k_{ji}x_j(t) - \sum_i \mu^k_i \sum_j k_{ij}x_i(t) \\ &= \sum_i \mu^k_i \sum_j \left[k_{ji}x_j(t) - k_{ij}x_i(t)\right] \\ &= \sum_i \mu^k_i \frac{\mathrm{d}}{\mathrm{d}t}x_i(t)\end{aligned} \tag{5}$$

In the last step, we used the relation $\frac{\mathrm{d}}{\mathrm{d}t}x_i(t) = \sum_j \left[k_{ji}x_j(t) - k_{ij}x_i(t)\right]$, which is the differential equation of the concentration $x_i(t)$, corresponding to the reactions of the ith intermediate.

As a result (using the simplified notation: $\mu^k(t) \stackrel{\mathrm{def}}{=} \tilde{\mu}^k(t)_\sum$) we obtain:

$$\mu^k(t) \sim \sum_i \mu^k_i \frac{\mathrm{d}}{\mathrm{d}t}x_i(t) \tag{6}$$

So the total dipole moment function of the system (all molecules + electrolyte) is proportional to the linear combination of the time derivatives of the intermediate concentrations, where the μ^k_i values are the proportionality factors. Note that the μ^k_i intermediate dipole moment is analogous to a quantity introduced as the "electrogenicity" of the ith intermediate (E_i) by Trissl (1990).

If the sample of perfect direction were realizable, the $\mu^k(t)$ functions could be obtained directly by monitoring the $u^k(t)$ far-field potential differences via properly aligned electrode pairs. In this far-field limit, multipole potentials can be neglected; therefore $u^k(t) \sim \mu^k(t)$ and the μ^k_i intermediate dipoles could then be determined using Eq. (6).

In this section we demonstrated how the μ^k_i intermediate dipole moments can be derived from the $\mu^k(t)$ functions. In the following we show how the $\mu^k(t)$ functions can be determined from the measured $u^k(t)$ functions in more realistic samples.

Sample of perfect orientation

In our description we use molecular and laboratory coordinate systems. If the protein to be studied (or the membrane containing it) has a permanent electric (or magnetic) dipole moment, it is possible to orient the molecules by using an electric (or magnetic) field. We define the molecular z axis by the permanent [or induced (discussed later)] dipole moment; the laboratory z axis is defined by the orientation axis; the x and y axes are unimportant at this point. The elementary μ^k_{ij} dipole moment changes coupled to conformational transitions will be constructively summed up in the orientation direction, resulting in a macroscopically detectable $\mu^z_L(t)$ total dipole moment, while the elementary charge movements in the perpendicular plane compensate each other:

$$\begin{aligned}\mu^z_L(t) &= \mu^z(t) \\ \mu^x_L(t) &= \mu^y_L(t) = 0\end{aligned} \tag{7}$$

To detect the x, y components, an asymmetry is needed in the x and y directions, too.

The case of photoselection

If the investigated molecular process is triggered by light absorption of a linear chromophore in the protein, it is possible to increase the asymmetry (transiently) by using linearly polarized light. The excitation probability is proportional to the scalar product square of the transition dipole moment of the chromophore and the exciting electric field vector. This direction-dependent activation by polarized light is called photoselection. Now we define the molecular y axis as the projection of the chomophore onto the plane perpendicular to z (the permanent dipole moment) (the x axis is derived from the requirement of a right-handed Cartesian coordinate

system) (Fig. 3a). Let us define the laboratory x axis by the excitation propagation axis (the y axis results from the right-handed coordinate system) (Fig. 3b). In the case of perfect orientation, the chromophores can be placed on a surface, the so-called chromophore cone having a half-angle β (Fig. 4a). The angle between the electric field vector of the exciting light and the laboratory z axis is denoted by α. For the excitation probability of a molecule with a molecular y axis making an angle γ with the laboratory y axis:

$$p(\alpha,\gamma) \sim [\vec{e}(\alpha)\vec{\mu}_{\mathrm{T}}(\gamma)]^2 \tag{8}$$

Here $\vec{\mu}_{\mathrm{T}}(\gamma)$ and $\vec{e}(\alpha)$ are unit vectors corresponding to the transition dipole moment of the chromophore and the electric field of the exciting light.

The projection of $\mu^k(t)$ onto the lth laboratory axis is:

$$\mu_{\mathrm{L}}^{lk}(\alpha,\gamma,t) \sim p(\alpha,\gamma)r^{lk}(\gamma)\mu^k(t) \tag{9}$$

where $r^{lk}(\gamma)$ is the matrix of rotation, which rotates the laboratory coordinate system into the molecular system.

Taking into account all molecules in the sample:

$$\mu_{\mathrm{L}}^{lk}(\alpha,t) \sim \int_0^{2\pi} \mu_{\mathrm{L}}^{lk}(\alpha,\gamma,t)\mathrm{d}\gamma \sim \int_0^{2\pi} p(\alpha,\gamma)r^{lk}(\gamma)\mu^k(t)\mathrm{d}\gamma$$

$$= \mu^k(t)\int_0^{2\pi} p(\alpha,\gamma)r^{lk}(\gamma)\mathrm{d}\gamma = \mu^k(t)f^{lk}(\alpha) \tag{10}$$

Calculating the $f^{lk}(\alpha) = \int_0^{2\pi} p(\alpha,\gamma)r^{lk}(\gamma)\mathrm{d}\gamma$ matrix, we obtain:

$$\left[f^{lk}(\alpha)\right] = \begin{bmatrix} \sim \sin 2\beta \sin 2\alpha & 0 & 0 \\ 0 & \sim \sin 2\beta \sin 2\alpha & 0 \\ 0 & 0 & f^{zz}(\alpha) \end{bmatrix} \tag{11}$$

This means that using photoselection it is possible to obtain the dipole moment functions $\mu^k(t)$ in the sample

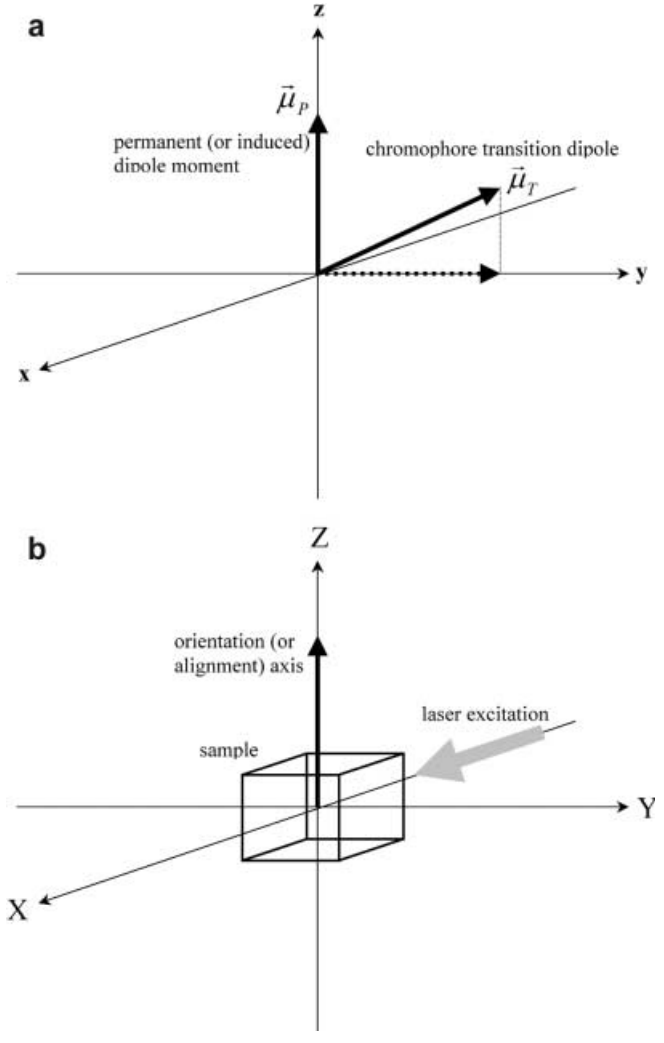

Fig. 3 Definition of the molecular (**a**) and laboratory (**b**) coordinate system

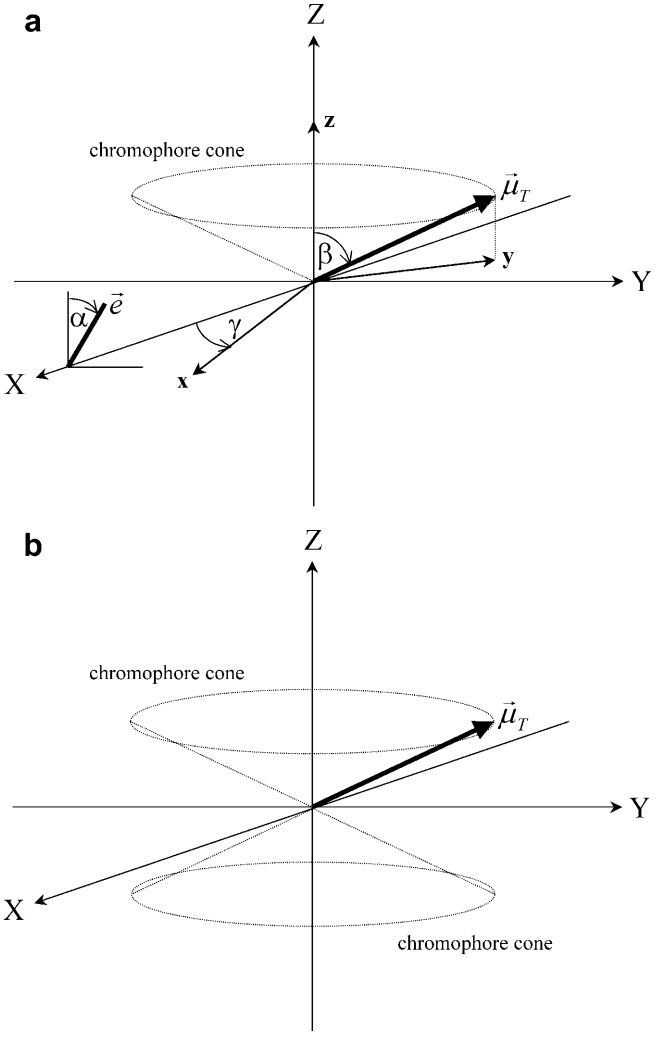

Fig. 4 The chromophore cone in the case of perfect orientation (**a**) and perfect alignment (**b**). $\vec{\mu}_{\mathrm{T}}$ is the transient dipole moment of the chromophore making a β angle with the z axis; the $\vec{e}$ electric field vector of the exciting light makes an angle α with the Z axis

of perfect orientation. The matrix is diagonal; thus the components $\mu^k(t)$ appear in the laboratory coordinate system separated on the corresponding axes. The function sin 2α has its extrema at $\alpha = 45°(+k\times 90°)$, so the projections of $\mu^x(t)$ and $\mu^y(t)$ have their maxima at $\alpha = 45°$ polarization angle (independent of β, the chromophore angle). It can be also easily seen that photoselection is most efficient with chromophores having $\beta = 45°$ (while in the extreme cases of $\beta = 0°$, 90° the photoselection effect disappears).

Sample of perfect alignment

Another type of symmetry can be realized in samples where the angular distribution of the molecules results from the interaction between an electric (or magnetic) field and its *induced* electric (or magnetic) dipoles. Here the molecular z axes are parallel with each other but their directions are random. The sample symmetry implies that the macroscopic scale dipole moment function of this system is zero:

$$\mu_{\mathrm{L}}^{k}(t) = 0 \tag{12}$$

The case of photoselection

If the molecules have a linear chromophore and polarized excitation is applied to trigger conformational changes, we have a more interesting case. The chromophores can be placed on two opposing chromophore cones (Fig. 4b). For every chromophore on the upper cone there is a chromophore on the lower cone with the same transition dipole vector, which are thus excited with the same probability. The two molecular coordinate systems corresponding to these chromophores can be transformed into each other with a 180° rotation around the molecular x axis. This means that the molecular y and z axes of the first molecule point in the opposite direction to the corresponding axes of the second one. So only dipole moment changes in the x molecular direction will be added constructively. Following a similar calculation as presented for the case of perfect orientation, we obtain:

$$\begin{aligned} &\mu_{\mathrm{L}}^{x}(t) \sim \mu^x(t) \sin 2\beta \sin 2\alpha \\ &\mu_{\mathrm{L}}^{k\neq x}(t) = 0 \end{aligned} \tag{13}$$

This means that the sample of perfect alignment offers the simplest way to obtain the $\mu^x(t)$ component.

Real samples

The sample of perfect orientation and perfect alignment – discussed previously – represent important theoretical cases, needed to understand real samples affected by the Boltzmann energy distribution. Here the molecules are gathered around an orientation (or alignment) axis, but not perfectly because their thermal energy acted against the orienting (or aligning) force when the angular distribution was fixed. This distribution depends on the type and strength of the orientation (or alignment) and can be described using the $\rho(\vartheta)$ angular density function, where ϑ is the angle made by the molecular and laboratory z axis (Fig. 2). Despite the more complicated angular distribution, it can be shown that, without photoselection, oriented samples also express only the $\mu^z(t)$ dipole component at the macroscopic level, similar to the sample of perfect orientation (Eq. 7), and no macroscopic dipole function is present at all in aligned samples, similar to the sample of perfect alignment (Eq. 12).

The case of photoselection

If photoselection is possible, one can also obtain the $\mu^x(t)$ and $\mu^y(t)$ components. In the case of aligned samples the angular distribution function is symmetric to $\vartheta = 90°$. Each chromophore cone corresponding to molecules having $\vartheta < 90°$ can be assigned to another chromophore cone with $\vartheta > 90°$ and having the same excitation probabilities. The sample can be composed of such cone pairs, and for each pair we have the case of the "sample of perfect alignment"; thus only the $\mu^x(t)$ dipole functions will be added constructively, resulting in a macroscopically detectable photovoltage. This means that these samples are ideal to obtain the unobscured $\mu^x(t)$, despite the complication of the Boltzmann distribution.

$\mu^z(t)$ can be determined using oriented samples, with isotropic excitation. In this case, all chromophores are excited with the same probability. Owing to the sample symmetry, only $\mu^z(t)$ will appear at the macroscopic level.

To determine the remaining $\mu^y(t)$ dipole function, more specific information on the sample symmetry is required. The direction of a molecular z axis (in the laboratory coordinate system) can be defined by two angles: ϑ and φ (the rotation angle around the orientation axis). The linear chromophore direction (in the laboratory coordinate system) can be defined by ϑ, φ and an additional angle γ, which is the rotation angle of the chromophore around the molecular z axis. For the excitation probability of the chromophore having (ϑ, φ, γ):

$$p_{\vec{e}}(\vartheta, \varphi, \gamma) \sim [\vec{e}\vec{\mu}_{\mathrm{T}}(\vartheta, \varphi, \gamma)]^2 \tag{14}$$

The molecules with a chromophore of (ϑ,φ,γ) produce a dipole moment proportional to $\rho(\vartheta) \times p_{\vec{e}}(\vartheta, \varphi, \gamma)$, so the projection of $\mu^k(t)$ onto the lth laboratory axis is given by:

$$\mu_{\mathrm{L}}^{lk}(t, \vartheta, \varphi, \gamma) \sim \rho(\vartheta) p_{\vec{e}}(\vartheta, \varphi, \gamma) r^{lk}(\vartheta, \varphi, \gamma) \mu^k(t) \tag{15}$$

where $r^{lk}(\vartheta,\varphi,\gamma)$ is the matrix of the (ϑ,φ,γ) rotation.

Taking into account all possible directions in the sample:

$$\mu_{\mathrm{L}}^{lk}(t) \sim \iiint_{\vartheta\varphi\gamma} \mu_{\mathrm{L}}^{lk}(t,\vartheta,\varphi,\gamma)\mathrm{d}\gamma\mathrm{d}\varphi\mathrm{d}\vartheta$$
$$\sim \iiint_{\vartheta\varphi\gamma} \rho(\vartheta)p_{\vec{e}}(\vartheta,\varphi,\gamma)r^{lk}(\vartheta,\varphi,\gamma)\mu^{k}(t)\mathrm{d}\gamma\mathrm{d}\varphi\mathrm{d}\vartheta$$
$$\sim \mu^{k}(t)\int_{\vartheta}\rho(\vartheta)\iint_{\varphi\gamma} p_{\vec{e}}(\vartheta,\varphi,\gamma)r^{lk}(\vartheta,\varphi,\gamma)\mathrm{d}\gamma\mathrm{d}\varphi\mathrm{d}\vartheta \tag{16}$$

which can be written in the form:

$$\mu_{\mathrm{L}}^{lk}(t) \sim \mu^{k}(t)f^{lk}(\rho,p_{\vec{e}}) \tag{17}$$

and finally the macroscopically detectable photovoltages $u^{l}(t)$:

$$u^{l}(t) \sim \mu_{\mathrm{L}}^{l}(t) = \sum_{k}\mu_{\mathrm{L}}^{lk}(t) \tag{18}$$

The matrix component $f^{lk}(\rho,p_{\vec{e}})$ can be thought of as the "weight" of $\mu^{k}(t)$ onto the lth laboratory axis. The values of these components can be calculated using numerical integration. Simulation software was created partly for this purpose, and the results showed (among others) that also in the oriented sample (affected by the Boltzmann distribution) photoselection is most effective at $\alpha = 45°$ excitation (similar to the case of perfect orientation); however on the laboratory y axis, $\mu^{y}(t)$ appears within a mixture containing $\mu^{z}(t)$:

$$u^{y}(t) \sim \mu_{\mathrm{L}}^{y}(t) \sim f^{yy}\mu^{y}(t) + f^{yz}\mu^{z}(t) \tag{19}$$

Based on the simulation, we give a method that delivers $\mu^{y}(t)$. The sample is excited at two polarization angles (α_1, α_2) and the corresponding $u^{y}{}_1(t)$ and $u^{y}{}_2(t)$ photovoltages are measured. In this case (eliminating irrelevant proportionality factors):

$$\begin{aligned} u_1^{y}(t) &= \mu^{y}(t) + \mu^{z}(t) \\ u_2^{y}(t) &= a\mu^{y}(t) + b\mu^{z}(t) \end{aligned} \tag{20}$$

where $a = \frac{f_2^{yy}}{f_1^{yy}}$ and $b = \frac{f_2^{yz}}{f_1^{yz}}$ can be obtained by numerical calculation knowing $\rho(\vartheta)$. From the equation system $\mu^{y}(t)$ can be derived (a perfect matching of the orientation axis, the excitation propagation axis and the photovoltage measuring directions is assumed).

Concept of evaluation

If the $\mu^{k}(t)$ traces are obtained from the measured $u^{k}(t)$ macroscopic voltages, and the $x_i(t)$ intermediate concentrations are available, one can calculate the μ_i^{k} intermediate dipole moments from Eq. (6). As this relation suggests, the μ_i^{k} values can only be determined up to the precision of unknown proportionality factors, different in the three spatial directions, due to the electrolyte relaxation process. However, the μ_i^{x}, μ_i^{y} and μ_i^{z} components do contain important information about charge rearrangements inside the molecule during its operation. Therefore their comparison with theoretically predicted data (molecular dynamics models) is of primary interest.

A molecular dynamics model usually contains both the structures of the intermediates and the so-called reaction graph (e.g. photocycle scheme in the case of bR). Using the reaction graph, the intermediate concentrations can be derived from absorption kinetic measurements. Then, from the photoelectric measurement, on the basis of Eq. (6) we can determine the μ_i^{k} values, that can be compared to the ones obtained directly from the intermediate structures. So the photoelectric measurement extended by absorption kinetic data offers the possibility to verify molecular dynamics results. Figure 5 shows the evaluation process.

For the correct interpretation of the μ_i^{k} values, it is important to remember that the dipole moment change for every transition is a superposition of the molecule conformation change and the optional intramolecular charge transport step.

In the case of a cyclic process, for the time integral of Eq. (6) we obtain:

$$\int_{\text{process}} \mu^{k}(t)\mathrm{d}t \sim \sum_{i=0}^{n}\mu_i^{k}\int_{\text{process}}\frac{\mathrm{d}}{\mathrm{d}t}x_i(t)\mathrm{d}t = \mu_n^{k} - \mu_0^{k} \tag{21}$$

which is expected to be zero, since the nth intermediate is the initial one. However, if the protein is a charge transporter, the first and last intermediates cannot be considered electronically equivalent, i.e. the dipole moment of the last intermediate differs from the initial one because of the transport process. If the transported charge has a total displacement of d^{k} inside the molecule, we can write:

$$\int_{\text{process}} \mu^{k}(t)\mathrm{d}t \sim \mu_n^{k} - \mu_0^{k} = qd^{k} \tag{22}$$

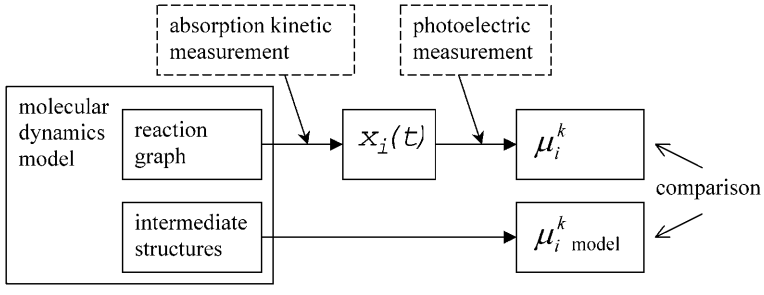

Fig. 5 Data evaluation diagram for the verification of molecular dynamics models based on the photoelectric measurement

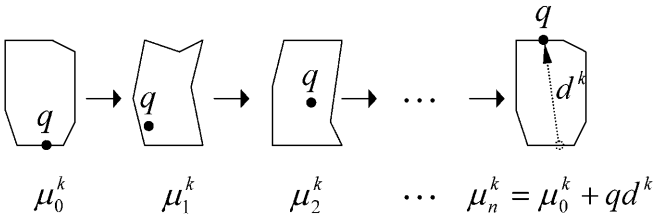

Fig. 6 Demonstration of the "electric" intermediates. The molecule conformation together with the transported charge defines the "electric" intermediate. The molecular conformations are symbolized with different polygons, while the transported charge (q) is represented by a *bold dot*; d^k is the total displacement of the charge inside the molecule

Figure 6 visualizes how the "electric" intermediates should be imagined. It is assumed that the diffusional motion of the transported charge in the electrolyte is non-electrogenic in the measuring system. Therefore, in the case of the first and last intermediates, the transported charge is considered to be on the surface of the molecule.

Miscellaneous remarks

As it was shown in the previous section, in the case of ion pumping processes of intramembrane proteins, the time integral of the $\mu^z(t)$ function (where z is parallel with the membrane normal) is proportional to the charge pumped across the membrane (Eq. 22), i.e. a "pumping efficiency" can be defined for the process investigated, having important implications (Dér et al. 1989, 1991; Keszthelyi and Ormos 1989).

At low ionic strengths, in the presence of special buffer molecules, the electric signals can be burdened by additional components, as has been shown in the case of bR (Marinetti 1987; Liu et al. 1990; Tóth-Boconádi et al. 2000). Our analysis is restricted to such cases where the contribution of buffer effects on the shape of the photovoltage is negligible. Even if buffer molecules are present in the solution, this is guaranteed whenever the salt concentration exceeds a critical limit (ca. 20 mM for monovalent and 3 mM for divalent cations) (Liu et al. 1990).

Another assumption implicitly used in the theory was non-saturational excitation at photoselection. In this case, photovoltages are proportional to the intensity of the exciting light.

Conclusions

The theory presented in this paper provides a comprehensive interpretation of electric signals measured by the suspension methods. The detailed analysis implies why electric signals can be utilized for the investigation of molecular ion pumps. They can be used to make distinction between the validity of different models (including reaction kinetics and molecule structures) of the investigated molecular process. Examples are presented in Dér et al. (1999). In general, they carry information about the underlying molecular processes, in addition to that which can be obtained from optical measurements. Absorption kinetic signals sometimes cannot be available at all, and in this case electric traces are the only source of information.

In addition to the investigation of intramolecular charge displacements in the pumping direction (Keszthelyi and Ormos 1980; Dér et al. 1992a; Sineshchekov et al. 1992; Ludmann et al. 1998), the full power of the suspension methods supported by this theory has been exploited in the case of bR, where electric dipole moment changes of the molecule could be derived in all three dimensions (Dér et al. 1999), giving important clues for the description of the pumping mechanism.

Acknowledgements The authors are indebted to Profs. Lajos Keszthelyi and György Váró for helpful discussions and critical reading of the manuscript. The work was supported by grants from the Hungarian research foundations: OTKA T-029814 and OTKA T-029764.

References

Barabás K, Dér A, Dancsházy Zs, Ormos P, Keszthelyi L, Marden M (1983) Electro-optical measurements on aqueous suspension of purple membrane from *Halobacterium halobium*. Biophys J 43:5–11

Dancsházy Z, Karvaly B (1976) Incorporation of bacteriorhodopsin into a bilayer lipid membrane; a photoelectric-spectroscopic study. FEBS Lett 72:136–138

Dér A, Fendler K, Keszthelyi L, Bamberg E (1985a) Primary charge separation in halorhodopsin. FEBS Lett 187:233–236

Dér A, Hargittai P, Simon J (1985b) Time-resolved photoelectric and absorption signals from oriented purple membranes immobilized in gel. J Biochem Biophys Methods 10:295–300

Dér A, Tóth-Boconádi R, Keszthelyi L (1989) Bacteriorhodopsin as a possible chloride pump. FEBS Lett 259:24–32

Dér A, Száraz S, Tóth-Boconádi R, Tokaji Zs, Keszthelyi L, Stoeckenius W (1991) Alternative translocation of protons and halide ions by bacteriorhodopsin. Proc Natl Acad Sci USA 88:4751–4755

Dér A, Tóth-Boconádi R, Száraz S (1992a) Electric signals and the photocycle of bacteriorhodopsin. Colloq INSERM 221:197–200

Dér A, Száraz S, Keszthelyi L (1992b) Charge displacements during the photocycle of halorhodopsin. J Photochem Photobiol B 15:299–306

Dér A, Tóth-Boconádi R, Keszthelyi L, Kramer H, Stoeckenius W (1995) Orientation of purple membrane in combined electric and magnetic fields. FEBS Lett 377:419–420

Dér A, Oroszi L, Kulcsár A, Zimányi L, Tóth-Boconádi R, Keszthelyi L, Stoeckenius W, Ormos P (1999) Interpretation of the spatial charge displacements in bacteriorhodopsin in terms of structural changes during the photocycle. Proc Natl Acad Sci USA 96:2776–2781

Drachev LA, Kaulen AD, Ostroumov SA, Skulachev VP (1974) Electrogenesis by bacteriorhodopsin incorporated in a planar phospholipid membrane. FEBS Lett 39:43–45

Fahr A, Läuger P, Bamberg E (1981) Photocurrent kinetics of purple-membrane sheets bound to planar bilayer membranes. J Membr Biol 60:51–62

Fowler CF, Kok B (1974) Direct observation of a light-induced electric field in chloroplasts. Biochim Biophys Acta 357:308–318

Govorunova E, Dér A, Tóth-Boconádi R, Keszthelyi L (1995) Photosynthetic charge separation in oriented membrane fragments immobilized in gel. Bioelectrochem Bioeng 38:53–56

Henderson R, Baldwin JM, Ceska TA, Zemlin F, Beckmann E, Downing KH (1990) An atomic model for the structure of bacteriorhodopsin. Biochem Soc Trans 18:844

Herrmann TR, Rayfield GW (1978) The electrical response to light of bacteriorhodopsin in planar membranes. Biophys J 21:111–125

Hong FT, Montal M (1979) Bacteriorhodopsin in model membranes. A new component of the displacement photocurrent in the microsecond time scale. Biophys J 25:465–472

Keszthelyi L (1980) Orientation of membrane fragments by electric field. Biochim Biophys Acta 598:429–436

Keszthelyi L, Ormos P (1980) Electric signals associated with the photocycle of bacteriorhodopsin. FEBS Lett 109:189–193

Keszthelyi L, Ormos P (1989) Protein electric response signals from dielectrically polarized systems. J Membr Biol 109:193–200

Liu SY, Ebrey TG (1988) Photocurrent measurements of the purple membrane oriented in a polyacrylamide gel. Biophys J 54:321–329

Liu SY, Govindjee R, Ebrey TG (1990) Light-induced currents from oriented purple membrane. II. Proton and cation contributions to the photocurrent. Biophys J 57:951–963

Ludmann K, Gergely C, Dér A, Váró G (1998) Electric signals during the bacteriorhodopsin photocycle, determined over a wide pH range. Biophys J 75:3120–3126

Marinetti T (1987) Counterion collapse and the effect of diamines on bacteriorhodopsin. FEBS Lett 216:155–158

Müller KH, Butt HJ, Bamberg E, Fendler K, Hess B, Siebert F, Engelhard M (1991) The reaction cycle of bacteriorhodopsin: an analysis using visible absorption, photocurrent and infrared techniques. Eur Biophys J 19:241–251

Ormos P, Dér A, Száraz S, Tokaji, Zs, Zimányi L, Nagy K (1996) Photoreactions and related charge displacements in the rhodopsin from *Sepia officinalis*. J Photochem Photobiol B 35:7–12

Sineshchekov OA, Govorunova EG, Dér A, Keszthelyi L, Nultsch W (1992) Photoelectric responses in phototactic flagellated algae measured in cell suspension. J Photochem Photobiol B 13:119–134

Tóth-Boconádi R, Dér A, Keszthelyi L (2000) Buffer effects on electric signals of light-excited bacteriorhodopsin. Biophys J 78:3170–3177

Trissl HW (1990) Photoelectric measurements of purple membranes. Photochem Photobiol 51:793–818

Trissl HW, Kunze U, Junge W (1982) Extremely fast photoelectric signals from suspension of broken chloroplasts and of isolated chromatophores. Biochim Biophys Acta 682:364–377

Váró G (1981) Dried oriented purple membrane samples. Acta Biol Acad Sci Hung 32:301–310

Váró G, Keszthelyi L (1983) Photoelectric signals from dried oriented purple membranes of *Halobacterium halobium*. Biophys J 43:47–51

Witt HT, Zickler A (1973) Electrical evidence for the field indicating absorption change in bioenergetic membranes. FEBS Lett 37:307–310